This is the accepted manuscript made available via CHORUS. The article has been published as:

Modulated Continuous Wave Control for Energy-Efficient Electron-Nuclear Spin Coupling

J. Casanova, E. Torrontegui, M. B. Plenio, J. J. García-Ripoll, and E. Solano

Phys. Rev. Lett. **122**, 010407 — Published 10 January 2019

DOI: 10.1103/PhysRevLett.122.010407

Modulated Continuous Wave Control for Energy-efficient Electron-nuclear Spin Coupling

J. Casanova,[1,2] E. Torrontegui,[3] M. B. Plenio,[4] J. J. García-Ripoll,[3] and E. Solano[1,2,5]

[1]*Department of Physical Chemistry, University of the Basque Country UPV/EHU, Apartado 644, 48080 Bilbao, Spain*
[2]*IKERBASQUE, Basque Foundation for Science, Maria Diaz de Haro 3, 48013 Bilbao, Spain*
[3]*Instituto de Física Fundamental IFF-CSIC, Calle Serrano 113b, 28006 Madrid, Spain*
[4]*Institut für Theoretische Physik and IQST, Albert-Einstein-Allee 11, Universität Ulm, D-89069 Ulm, Germany*
[5]*Department of Physics, Shanghai University, 200444 Shanghai, China*

We develop energy efficient, continuous microwave schemes to couple electron and nuclear spins, using phase or amplitude modulation to bridge their frequency difference. These controls have promising applications in biological systems, where microwave power should be limited, as well as in situations with high Larmor frequencies due to large magnetic fields and nuclear magnetic moments. These include nanoscale NMR where high magnetic fields achieves enhanced thermal nuclear polarisation and larger chemical shifts. Our controls are also suitable for quantum information processors and nuclear polarisation schemes.

Introduction.– Color centers in diamond, such as the nitrogen-vacancy (NV) center [1, 2], have emerged as a solid state system that can detect, polarise and control individual nuclear spins in their vicinity [3–6]. This ability promises applications that range from quantum information processing and quantum simulation on small scale quantum registers [7–13] to nanoscale nuclear magnetic resonance (NMR) [14–16] and other sensing tasks in biological environments [17]. A fundamental question in this field is how to extend the coherence time of color centers —insulating them from their fluctuating magnetic environment—, while enabling strong and selective interactions with individual nuclear spins. For the NV center this challenge is met through dynamical decoupling (DD) schemes: continuous [18–21] or pulsed microwave sequences [10, 22–31] that can be applied to mitigate the impact of solid state [32–34] and biological environments [35, 36].

In the context of NMR e.g., the presence of strong magnetic fields would be of great benefit as they increase the NMR signal by enhancing the spin polarisation, induce large chemical shifts that encode molecular structure [37], and aid in the spectral resolution of spins. Moreover, strong magnetic fields lead to longer nuclear spin lifetimes, facilitating quantum information processors and nuclear polarisation schemes.

Nevertheless, experiments with color centers are typically realised in the sub-Tesla magnetic field regime [4, 8, 9, 11, 38–48] due to experimental limitations. The obstacle is the need to bridge the frequency mismatch between the NV center and the target spin in the presence of a high externally applied magnetic field. When using continuous microwaves, the Larmor frequency of the target nucleus determines the Rabi frequency of the microwave control —the Hartmann-Hahn (HH) condition [49]—, implying microwave powers that grow with the magnetic field and imposing serious stability requirements on the microwave source. The situation does not improve for pulsed controls: the Larmor frequency determines the frequency at which π-pulses are applied to the color center, implying very fast and energetic pulses with high-frequency repetition rates. These power requirements also imply significant challenges for their use in biological samples, because a strong microwave heats the organic matter, perturbing its dynamics or even destroying it. In recent work this challenge was identified and addressed [50]. However, in microwave power sensitive applications continuous wave may offer advantages as their average energy consumption at the same decoupling and sensing efficiency can be lower than for pulsed schemes [36].

In this Letter, we show that there are indeed continuous microwave controls that can bridge the Larmor frequency difference between electronic and nuclear spins. These methods modulate the phase or amplitude of a continuous microwave field. The modulation is taken to have a frequency $\nu \sim \omega_n - \Omega_0$ that provides the difference between the Rabi frequency of the microwave pulse Ω_0 and the frequency of the target nuclear spin ω_n. This technique works even when the microwave field amplitude Ω_0 is insufficient to achieve a HH resonance. As a result, our schemes demand lower peak and average powers to achieve a coherent interaction with a nucleus than all continuous controls based on the HH condition. Furthermore, we demonstrate that, thanks to the periodic modulation scheme, our controls inherit the robustness against control errors that is typical of DD and pulsed methods.

We start by considering the Hamiltonian of an NV electron spin coupled to a set of nuclei. This reads ($\hbar = 1$)

$$H = DS_z^2 - \gamma_e B_z S_z - \sum_j \gamma_j B_z I_z + S_z \sum_j \vec{A}_j \cdot \vec{I}_j + H_c, \quad (1)$$

with the NV zero-field splitting $D = (2\pi) \times 2.87$ GHz, a constant magnetic field B_z applied along the NV axis (i.e. the $\hat{z}$ axis), the gyromagnetic constants for the electronic spin $\gamma_e \approx -(2\pi) \times 28.024$ GHz/T and specific nuclei in the environment γ_j —e.g. ^{13}C nuclei have $\gamma_{^{13}\mathrm{C}} = (2\pi) \times 10.705$ MHz/T—. The NV spin operators are $S_z = |1\rangle\langle 1| - |-1\rangle\langle -1|$ and $S_x = 1/\sqrt{2}(|1\rangle\langle 0| + |-1\rangle\langle 0| + \mathrm{H.c.})$. The hyperfine vector decays according to a dipole-dipole interaction [51] $\vec{A}_j = \frac{\mu_0 \gamma_e \gamma_n}{2|\vec{r}_j|^3}[\hat{z} - 3\frac{(\hat{z}\cdot\vec{r}_j)\vec{r}_j}{|\vec{r}_j|^2}]$ with the vector $\vec{r}_j$ connecting the NV center and the jth nucleus. The microwave (MW) control Hamiltonian is conveniently written as $H_c = \sqrt{2}\Omega S_x \cos(\omega t - \phi)$, parametrized by two external controls: the Rabi frequency Ω and the microwave phase ϕ, while the MW frequency ω will be on resonance with one of the NV spin transitions, namely the $|0\rangle \leftrightarrow |1\rangle$ transition [52]. Hamiltonian (1) should include

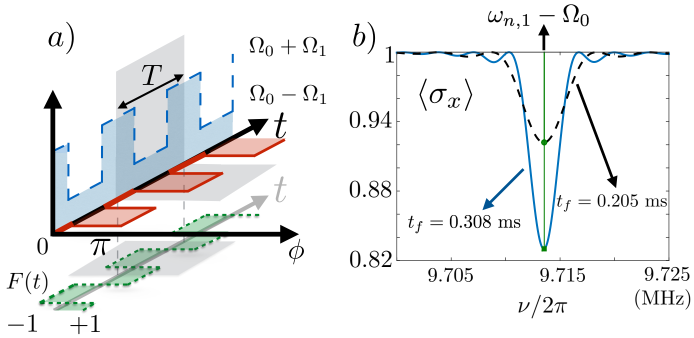

FIG. 1. a) A discrete phase modulation in time $\phi(t)\in\{0,\pi\}$ (red-solid line) combined with a constant drive, leads to modulations of the Rabi frequency $\Omega(t)=\Omega_0+F(t)\Omega_1\in\{\Omega_0-\Omega_1,\Omega_0+\Omega_1\}$ (blue long-dashed line). Modulation function $F(t)$ (green short-dashed line). b) Harvested signal $\langle\sigma_x\rangle$ vs. phase modulation frequency $\nu=2\pi/T$ for two interrogation times, $t_f=0.205$ ms (black-dashed line) and $t_f=0.308$ ms (blue-solid line). Signal is maximal when $\nu=\omega_{n,1}-\Omega_0$ spans the difference between the Rabi frequency of the NV and the resonance frequency of the interrogated nuclear spin.

the dipole-dipole interaction among nuclei. We omit it to simplify the presentation but it will be fully considered in the numerical simulations below.

An external magnetic field and a suitably tuned microwave field effectively reduce the dimensionality of the NV-center, which can be treated as a pseudospin. The new Hamiltonian [52]

$$H=-\sum_j\omega_{n,j}\,\hat{\omega}_{n,j}\cdot\vec{I}_j+\frac{\sigma_z}{2}\sum_j\vec{A}_j\cdot\vec{I}_j+\frac{\Omega}{2}(|1\rangle\langle 0|\,e^{i\phi}+\text{H.c.}) \tag{2}$$

is defined in a rotating frame generated by $H_0=DS_z^2-\gamma_e B_z S_z$. In this frame, the jth nuclear spin's resonance frequency $\omega_{n,j}=|\vec{\omega}_{n,j}|$ with $\vec{\omega}_{n,j}=(-\frac{1}{2}A_{x,j},-\frac{1}{2}A_{y,j},\omega_{\rm L}-\frac{1}{2}A_{z,j})$ depends on the hyperfine vectors and the nuclear Larmor frequency $\omega_{\rm L}=\gamma_j B_z$. For simplicity we assume a cluster of ^{13}C nuclei $\gamma_j=\gamma_{^{13}\text{C}}\ \forall j$ (a common situation in diamond samples) and introduce the normalized vectors $\hat{\omega}_{n,j}=\vec{\omega}_{n,j}/\omega_{n,j}$. When the magnetic field B_z is large, the resonance frequency of the jth nucleus deviates linearly from its Larmor frequency $\omega_{\rm L}$ as a function of the hyperfine vector

$$\omega_{n,j}\approx\omega_{\rm L}-\frac{1}{2}A_{z,j}\equiv\gamma_{^{13}\text{C}}B_z-\frac{1}{2}A_{z,j}. \tag{3}$$

The HH condition [49] is a standard procedure to achieve resonant interaction with a nuclear spin (e.g. the jth one) in which the Rabi frequency matches the frequency of the target spin $\Omega=\omega_{n,j}=\gamma_{^{13}\text{C}}B_z-\frac{1}{2}A_{z,j}$. In high-field environments this implies large Rabi frequencies and microwave powers — e.g. $B=1$ T gives $\Omega/(2\pi)\approx 10$ MHz for a ^{13}C and 42 MHz for a ^{1}H nucleus—. Our goal is to lower these requirements with minor changes in the control field.

Phase modulation control scheme.– We address this challenge and enable NV-nuclear coupling at high magnetic fields by introducing a continuous drive in Eq. (1) described by

$$H_{\rm c}=\sqrt{2}\Omega_0 S_x\cos(\omega t)+\sqrt{2}\Omega_1 S_x\cos(\omega t-\phi), \tag{4}$$

with a phase ϕ that will be switched periodically between the values 0 and π. The control in Eq. (4) gives rise to the following Hamiltonian that we will use as the starting point of our simulations [52]

$$H=-\sum_j\omega_{n,j}\hat{\omega}_{n,j}\cdot\vec{I}_j+\frac{\sigma_z}{2}\sum_j\vec{A}_j\cdot\vec{I}_j+\left(\frac{\Omega_0+\Omega_1 e^{i\phi}}{2}\,|1\rangle\langle 0|+\text{H.c.}\right). \tag{5}$$

For the sake of clarity of presentation we consider the phase flips as instantaneous, but stress that in our numerical simulations the phase flips will take a finite time determined by experimental limitations. In Eq. (5) the phase flip between 0 and π allows to write the driving term, i.e. the last term at its right hand side, as $[(\Omega_0+F(t)\ \Omega_1)/2\,|1\rangle\langle 0|+\text{H.c.}]$ where the modulation function $F(t)$ takes the values $+1$ (or -1) for $\phi=0$ (or $\phi=\pi$). Control of the phase allows for the construction of a modulation function $F(t)$ with period T, see Fig. 1(a), that can be expanded in its Fourier components as $F(t)=\frac{a_0}{2}+\sum_{n=1}^{\infty}\left[a_n\cos\left(\frac{2n\pi}{T}t\right)+b_n\sin\left(\frac{2n\pi}{T}t\right)\right]$ where $a_n=\frac{2}{T}\int_0^T F(t)\cos\left(\frac{2n\pi}{T}t\right)$, and $b_n=\frac{2}{T}\int_0^T F(t)\sin\left(\frac{2n\pi}{T}t\right)$.

To determine the NV-nuclear coupling mechanism and the required resonance condition that result from the phase control in Eq. (4) we move to a rotating frame with respect to $-\sum_j\omega_{n,j}\,\hat{\omega}_{n,j}\cdot\vec{I}_j$ and the driving term $[(\Omega_0+F(t)\,\Omega_1)/2\,|1\rangle\langle 0|+$ H.c.]. For simplicity we select a phase change that produces an even $F(t)$, i.e. $F(t)=\sum_{n=1}^{\infty}a_n\cos(n\nu t)$ where $\nu=2\pi/T$ but other constructions including odd components for $F(t)$ are equally possible. This leads to the Hamiltonian [52]

$$H(t)=\frac{1}{2}\left[|+\rangle\langle -|e^{i\Omega_0 t}e^{i\sum_{n=1}^{\infty}\frac{a_n\Omega_1}{n\nu}\sin(n\nu t)}+\text{H.c.}\right]\cdot$$
$$\sum_j\left[A_{x,j}^{\perp}I_{x,j}\cos(\omega_{n,j}t)+A_{y,j}^{\perp}I_{y,j}\sin(\omega_{n,j}t)+A_{z,j}^{\parallel}I_{z,j}\right], \tag{6}$$

where $|\pm\rangle=\frac{1}{\sqrt{2}}(|1\rangle\pm|0\rangle)$, $A_{x,j}^{\perp}=|\vec{A}_j-(\vec{A}_j\cdot\hat{\omega}_{n,j})\ \hat{\omega}_{n,j}|$, $A_{y,j}^{\perp}=|\hat{\omega}_{n,j}\times\vec{A}_j|$, $A_{z,j}^{\parallel}=|(\vec{A}_j\cdot\hat{\omega}_{n,j})\ \hat{\omega}_{n,j}|$, $I_{\delta,j}=\vec{I}_j\cdot\hat{\delta}$ with $\hat{\delta}=\hat{x}_j,\ \hat{y}_j$, or $\hat{z}_j$, and $\hat{x}_j=\frac{\vec{A}_j-(\vec{A}_j\cdot\hat{\omega}_{n,j})\ \hat{\omega}_{n,j}}{A_x^{\perp}}$, $\hat{y}_j=\frac{\hat{\omega}_{n,j}\times\vec{A}_j}{A_y^{\perp}}$, $\hat{z}_j=\frac{(\vec{A}_j\cdot\hat{\omega}_{n,j})\ \hat{\omega}_{n,j}}{A_{z,j}^{\parallel}}$. With the aid of the Jacobi-Anger expansion ($e^{iz\sin(\theta)}\equiv\sum_{n=-\infty}^{+\infty}J_n(z)\ e^{in\theta}$, with $J_n(z)$ the Bessel function of the first kind) we can rewrite the exponentials in Eq. (6) as $e^{i\Omega_0 t}e^{i\sum_{n=1}^{\infty}\frac{a_n\Omega_1}{n\nu}\sin(n\nu t)}=\prod_{n=1}^{\infty}\sum_{m=-\infty}^{\infty}J_m\left(\frac{a_n\Omega_1}{n\nu}\right)e^{i(\Omega_0+mn\nu)t}$ to find

$$\Omega_0+mn\nu=\omega_{n,k} \tag{7}$$

as the resonance condition for the kth nucleus [52]. Equation (7) implies that, unlike the HH condition, an NV-nucleus resonance can be achieved for small Rabi frequencies Ω_0, Ω_1 if we apply a continuous drive interrupted by periodic phase flips at a large frequency ν. Equation (7) exhibits resonances for a wide variety of values m and n but for small arguments $a_n\Omega_1/(n\nu)$ the interaction strength between the NV and the kth nucleus is largest for $m = n = 1$ and $\nu = \omega_{n,k} - \Omega_0$ which yields the effective NV-nucleus flip-flop Hamiltonian [52]

$$H \approx \frac{A^{\perp}_{x,k}}{2} J_1\left(\frac{a_1\Omega_1}{\nu}\right)\left[\,|+\rangle\langle -|I^{+}_{k} + |-\rangle\langle +|\,I^{-}_{k}\right]. \tag{8}$$

For the discussion of the energy efficiency it is important to stress at this point that, as we will demonstrate later, a large value for ν does not imply large microwave power.

The Hamiltonian (8) produces a signal that we will quantify with the electronic expectation value $\langle\sigma_x\rangle$, with $\sigma_x = |1\rangle\langle 0| + |0\rangle\langle 1|$. More specifically, from Eq. (8) one can calculate that the expected signal for a sequence of length t_f is

$$\langle\sigma_x\rangle = \cos^2\left[\frac{A^{\perp}_{x,k} J_1(a_1\Omega_1/\nu)}{4} t_f\right]. \tag{9}$$

Note that, for a periodic phase-modulated sequence as the one showed in Fig. 1(a) we have $a_1 = 4/\pi$. Finally, we would like to remark that continuous DD schemes with periodic phase flips have been proposed for extending the NV coherence [53] and to improve DD robustness [20], but their advantages in terms of energy efficiency and nuclear spin control have not been explored to the best of our knowledge.

Amplitude modulation control scheme.– As an alternative to phase modulation we may also consider amplitude modulation for achieving energy-efficient electron-nuclear coupling. Let us consider an amplitude modulated continuous driving field of the form

$$H_c = \sqrt{2}\Omega(t) S_x \cos(\omega t) \tag{10}$$

with $\Omega(t) = \Omega_0 - \Omega_1 \sin(\nu t)$. Analogously to the previous section (for more details see [52]) we find $H(t) = \frac{1}{2}\left[\,|+\rangle\langle -|e^{i\Omega_0 t} e^{i\frac{\Omega_1}{\nu}\cos(\nu t)} + \text{H.c.}\right]\cdot \sum_j \left[A^{\perp}_{x,j} I_x \cos(\omega_{n,j} t) + A^{\perp}_{y,j} I_{y,j} \sin(\omega_{n,j} t) + A^{\parallel}_{z,j} I_z\right]$. While we selected an odd amplitude modulation, i.e. a sine-like tailoring for Ω_1, we would like to stress that other combinations including even modulations are also possible. Again, using the Jacobi-Anger expansion, $e^{iz\cos(\theta)} \equiv J_0(z) + 2\sum_{n=1}^{+\infty} i^n J_n(z)\cos(n\theta)$, we find for $\nu = \omega_{n,k} - \Omega_0$ the following flip-flop Hamiltonian between the NV and the kth nucleus [52] $H \approx \frac{A^{\perp}_{x,k}}{2} J_1\left(\frac{\Omega_1}{\nu}\right)\left[i\,|+\rangle\langle -|\,I^{+}_{k} - i\,|-\rangle\langle +|\,I^{-}_{k}\right]$, that leads to $\langle\sigma_x\rangle = \cos^2\left[\frac{A^{\perp}_{x,k} J_1(\Omega_1/\nu)}{4} t_f\right]$.

Numerical verification.– In the following we will analyse the phase-modulated scheme numerically to verify the accuracy of the theoretical analysis (see [52] for the analysis of the amplitude modulated scheme which yields similar results). This provides two alternatives which, depending on the specifics of the experimental equipment and the physical set-up, can be chosen for optimal performance in practice.

To demonstrate the performance of the method, in Fig. 1(b) we show a spectrum involving an NV center and a single ^{13}C nucleus such that $\vec{A} \approx (2\pi) \times [-6.71, 11.62, -17.09]$ kHz and $B = 1$ T which results in a nuclear Larmor frequency of $\approx (2\pi)\times 10$ MHz. This hyperfine vector $\vec{A}$ corresponds to a ^{13}C nucleus located in one available position of a diamond lattice. We used two phase-modulated sequences of different duration (see caption for more details) and show that the obtained signals (yellow-solid and black-dashed curves) that were numerically computed from Eq. (5) match, firstly, the position of the expected resonance $\nu = \omega_{n,1} - \Omega_0$ for $m = n = 1$, see Eq. (7), and, secondly, the theoretically calculated depth (green vertical lines with the circle and square denoting the maximum theoretical depth) for the signal $\langle\sigma_x\rangle$, see Eq. (9), for two different evolution times. Furthermore, in our numerical simulations we did not assume instantaneous 0 to π phase flips but allowed the phase change to take place in a time interval of length $t_{\phi_{\text{flip}}} \approx 5$ ns, with ϕ changing from 0 to π in 20 discrete steps which is well within the reach of the time-resolution of modern arbitrary waveform generators [54]. To calculate the signals in Fig. 1(b) we used Rabi frequencies $\Omega_0 = \Omega_1 = (2\pi) \times 1$ MHz which are one order of magnitude below the Rabi frequency that would achieve a HH resonance and concomitantly more energy efficient. Furthermore, our phase modulated scheme allows us to get narrower signals than those obtained with the HH scheme, see Ref. [52].

Nuclear spin addressing and robustness.– Our method also offers the possibility of improving nuclear spin addressing by modifying the value of Ω_1. Hamiltonian (8) shows that the effective NV-nuclear coupling is given by $A^{\perp}_{x,k}/2\ J_1(a_1\Omega_1/\nu) \approx A^{\perp}_{x,k}/2\left(\frac{a_1\Omega_1}{2\nu}\right)$. Then, a lower value Ω_1 implies a longer evolution and better energy selectivity as the rotating wave approximation over non-resonant terms is more accurate [52]. In addition, fluctuations on the microwave control are also reduced. Note that these are proportional to the Rabi frequency, i.e. $\Omega_{0,1}$ should be replaced by $\Omega_{0,1}[1 + \xi(t)]$ with $\xi(t)$ a fluctuating function. We will show the robustness of our scheme in the face of realistic control errors, see later in Fig. 2. Furthermore, in Ref. [52] we study situations with even larger control error conditions, as well as a comparison with the error accumulation process for the case of the HH resonance.

For the case of NV centers in diamonds with a low Nitrogen concentration, i.e. in ultrapure diamond samples, the main source of decoherence appears as a consequence of the coupling among the NV center and the ^{13}C nuclei in the lattice [51, 55]. In Fig. 2 we have simulated a system containing an NV quantum sensor and a three coupled ^{13}C nuclear spin cluster in a diamond lattice. The hyperfine vectors of the simulated sample are $\vec{A}_1 \approx (2\pi) \times [-6.71, 11.62, -17.09]$ kHz, $\vec{A}_2 \approx (2\pi) \times [-8.21, 23.70, -34.30]$ kHz, and $\vec{A}_3 \approx (2\pi) \times [6.76, 19.53, -8.02]$ kHz, such that the resonant frequencies at $B = 1$ T, see Eq. (3), are $\omega_{n,1} = (2\pi) \times 10.71$ MHz, $\omega_{n,2} = (2\pi) \times 10.72$ MHz, and $\omega_{n,3} = (2\pi) \times 10.70$ MHz. These nuclei present internuclear coupling coefficients $g_{j,l} = (\mu_0/4)(\gamma^2_{^{13}\text{C}}/r^3_{j,l})[1 - 3(n^z_{j,l})^2]$ (with $r_{j,l}$ the distance between jth and lth nuclei, and $n^z_{j,l}$ the z-projection

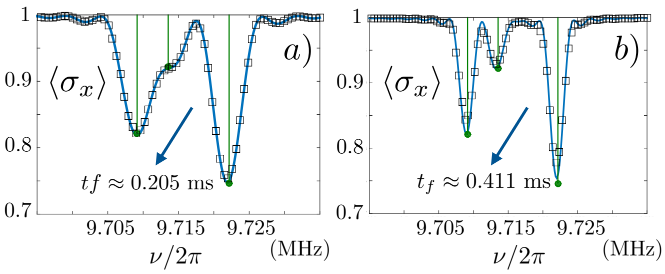

FIG. 2. Harvested signal $\langle\sigma_x\rangle$ as function of ν for ideal phase-modulated sequences (blue-solid curves) and for a situation that involves fluctuations of the microwave amplitude (black squares). The microwave amplitude fluctuation has been simulated with a OU process, while the black squares have been computed by averaging the results that correspond to 200 experiments. In a) we used $\Omega_0 = \Omega_1 = (2\pi) \times 1$ MHz, while in b) $\Omega_0 = (2\pi) \times 1$ MHz and $\Omega_1 = (2\pi) \times 0.5$ MHz.

of the unit vector $\vec{r}_{j,l}/r_{j,l}$) that are $g_{1,2} \approx (2\pi) \times -472$ Hz, $g_{1,3} \approx (2\pi) \times 14.95$ Hz, and $g_{2,3} \approx (2\pi) \times 50.10$ Hz. In Fig. 2(a) we use a phase-modulated continuous sequence with $\Omega_0 = \Omega_1 = (2\pi) \times 1$ MHz for a final time $t_f = 0.205$ ms. Here, we have simulated an ideal phase-modulated sequence without microwave control errors (blue-solid line) and a situation involving microwave power fluctuations (black squares). It can be observed that both signals overlap, i.e. the method is noise resilient while, both, the position of the resonances and the depth of of the signals (green vertical lines) coincide with the theoretical prediction of Eqs. (3) and (9), respectively. The noise in the microwave field is simulated by averaging 200 runs of a Ornstein-Uhlenbeck (OU) stochastic process [56] with time correlation $\tau = 0.5$ ms and noise amplitude $p = 0.5\%$ [57]. In Fig. 2(a) the three spin resonances cannot be fully resolved, however in Fig. 2(b) we used a different set of control parameters, namely $\Omega_0 = (2\pi) \times 1$ MHz, $\Omega_1 = (2\pi) \times 0.5$ MHz and a longer sequence $t_f = 0.411$ ms. In these conditions the effective NV-coupling has been reduced by a factor of 2 (note that we are also implementing a longer sequence) as the corresponding Bessel functions are $J_1(a_1[(2\pi) \times 0.5\text{MHz}]/\nu) \approx \frac{1}{2} J_1(a_1[(2\pi) \times 1\text{MHz}]/\nu)$, and the three nuclear spins can be clearly resolved. Again, the blue solid line represent the ideal signal while overlapping black squares have been calculated under the same noise conditions than the previous case.

Summarizing, from Fig. 2(b) we can observe how our phase-modulated driving preserves a coherent NV-target nucleus interaction, while eliminating the contributions of the rest of spins in the cluster. Hence, our DD scheme is able to efficiently average-out noisy signals from environmental spins, for more details see Ref. [52].

Power consumption.– Using phase (or amplitude) modulations leads to a reduction in the microwave field amplitude, i.e. in the peak power, and may be even lead to a reduction in the average power, as compared to other controls using the HH condition. We can quantify the average power reduction comparing the phase modulation scheme with a constant drive based on the HH condition (note that the peak power reduction is obvious as the largest driving we are using is $(2\pi) \times 1$ MHz which is approximately one order of magnitude smaller than the required driving to hold the HH condition). For that we first identify the times t_f^{ph} and t_f^{HH} for phase modulation and constant HH controls to gather the same signal $\langle\sigma_x\rangle$. With this information, we can compute the average power or energy flux associated to the microwave control [52].

Let us do the calculation: the protocol with constant amplitude produces a nuclear signal $\langle\sigma_x\rangle = \cos^2(A_{x,k}^{\perp} t_f^{HH}/4)$ in a time t_f^{HH}. Comparing with Eq. (9) we find that, for equal signals, the unmodulated protocol implements a faster interaction in a time $t_f^{HH} = J_1(a_1\Omega_1/\nu) t_f^{ph} < t_f^{ph}$. During this time, the constant driving scheme requires a Rabi frequency $\bar{\Omega}_0 = \omega_{n,k} = \Omega_0 + \nu$ to interact with the k-th nucleus with frequency $\omega_{n,k}$. This implies an average energy per cycle $E_T^{HH} \approx \bar{\Omega}_0^2/\nu$. The phase modulated protocol, on the other hand, requires an average energy per cycle $E_T^{ph} \sim (\Omega_0^2 + \Omega_1^2)/\nu$. Counting the number of cycles in the respective interaction times t_f^{HH} and t_f^{ph}, we obtain the ratio between total powers $E^{HH}/E^{ph} = \nu t_f^{HH} E_\nu^{HH}/(\nu t_f^{ph} E_\nu^{ph}) = (\Omega_0+\nu)^2 J_1(a_1\Omega_1/\nu)/(\Omega_0^2+\Omega_1^2)$. We can simplify this formula assuming fast modulation $\nu \gg \Omega_0, \Omega_1$ and approximating $J_1(a_1\Omega_1/\nu) \sim a_1\Omega_1/(2\nu)$. The result is that the phase modulated protocol demands significantly less energy $E^{HH}/E^{ph} \approx (\Omega_0 + \nu)^2 \Omega_1 a_1/[2\nu(\Omega_0^2 + \Omega_1^2)] \gg 1$. For the parameters used in Figs. 2(a) and (b), one finds $E^{HH}/E^{ph} \simeq 3.8$ and $E^{HH}/E^{ph} \simeq 3.0$, respectively, illustrating the efficiency of our method. A similar calculation can be done for the amplitude modulation protocol.

Conclusions.– We have proposed to use amplitude or phase modulation for coupling electron and nuclear spins at Rabi frequencies well below the Hartmann-Hahn resonance. Our schemes demand lower peak and average power to achieve the same sensitivity. As a consequence, these methods can be employed for sensing, coherent control, and nuclear polarisation with limited accessible power. In particular, they enable the operation of such sensors at high magnetic fields with reduced power. These modulation techniques extend nanoscale NMR techniques to biological systems that are sensitive to heating by microwaves. Moreover, these parametric methods are not specific to the NV center; they can be used to couple different electron spins to proximal nuclear spins, both in solid and molecular samples.

E.S. and J.C. acknowledge financial support from Spanish MINECO/FEDER FIS2015-69983-P, Basque Government IT986-16, as well as from QMiCS (820505) and OpenSuperQ (820363) of the EU Flagship on Quantum Technologies. J.C. acknowledges support by the Juan de la Cierva grant IJCI-2016-29681. E.T. and J.J.G.R. acknowledge support from Spanish MINECO/FEDER Project FIS2015-70856-P, FIS2016-81891-REDT and CAM PRICYT project QUITEMAD+CM S2013-ICE2801. M.B.P. acknowledges support by the ERC Synergy grant BioQ (grant no 319130), the EU project HYPERDIAMOND, the QuantERA project

NanoSpin, the BMBF project DiaPol, the state of Baden-Württemberg through bwHPC, and the German Research Foundation (DFG) through grant no INST 40/467-1 FUGG. This material is also based upon work supported by the U.S. Department of Energy, Office of Science, Office of Advance Scientific Computing Research (ASCR), Quantum Algorithms Teams project under field work proposal ERKJ335.

[1] M. W. Doherty, N. B. Manson, P. Delaney, F. Jelezko, J. Wrachtrup, and L. C. L. Hollenberg, Phys. Rep. **528**, 1 (2013).
[2] V. V. Dobrovitski, G. D. Fuchs, A. L. Falk, C. Santori, and D. D. Awschalom, Annu. Rev. Condens. Matter Phys **4**, 23 (2013).
[3] F. Jelezko, T. Gaebel, I. Popa, A. Gruber and J. Wrachtrup. Phys. Rev. Lett. **92**, 076401 (2004).
[4] C. Müller, X. Kong, J.-M. Cai, K. Melentijević, A. Stacey, M. Markham, D. Twitchen, J. Isoya, S. Pezzagna, J. Meijer, J. F. Du, M. B. Plenio, B. Naydenov, L. P. McGuinness, and F. Jelezko, Nat. Commun **5**, 4703 (2014).
[5] P. London, J. Scheuer, J.-M. Cai, I. Schwarz, A. Retzker, M. B. Plenio, M. Katagiri, T. Teraji, S. Koizumi, J. Isoya, R. Fischer, L. P. McGuinness, B. Naydenov, and F. Jelezko. Phys. Rev. Lett. **111**, 067601 (2013).
[6] R. Fischer, C.O. Bretschneider, P. London, D. Budker, D. Gershoni, and L. Frydman, Phys. Rev. Lett. **111**, 057601 (2013).
[7] J. M. Cai, A. Retzker, F. Jelezko, and M. B. Plenio. Nature Phys. **9**, 168 (2013).
[8] T. H. Taminiau, J. Cramer, T. van der Sar, V. V. Dobrovitski, and R. Hanson, Nat. Nanotechnol. **9**, 171 (2014).
[9] G. Waldherr, Y. Wang, S. Zaiser, M. Jamali, T. Schulte-Herbrüggen, H. Abe, T. Ohshima, J. Isoya, J. F. Du, P. Neumann, and J. Wrachtrup, Nature **506**, 204 (2014).
[10] J. Casanova, Z.-Y. Wang, J. F. Haase, and M. B. Plenio, Phys. Rev. A **92**, 042304 (2015).
[11] J. Cramer, N. Kalb, M. A. Rol, B. Hensen, M. S. Blok, M. Markham, D. J. Twitchen, R. Hanson, and T. H. Taminiau, Nat. Commun. **7**, 11526 (2016).
[12] J. Casanova, Z.-Y. Wang, and M. B. Plenio, Phys. Rev. Lett. **117**, 130502 (2016).
[13] M. A. Perlin, Z.-Y. Wang, J. Casanova, and M. B. Plenio, Quantum Sci. Technol. 4, 015007 (2018).
[14] S. Schmitt, T. Gefen, F. M. Stürmer, T. Unden, G. Wolff, Ch. Müller, J. Scheuer, B. Naydenov, M. Markham, S. Pezzagna, J. Meijer, I. Schwarz, M. B. Plenio, A. Retzker, L. P. McGuinness, and F. Jelezko, Science **351**, 832 (2017).
[15] J. M. Boss, K.S. Cujia, J. Zopes, and C. L. Degen, Science **351**, 837 (2017).
[16] D. R. Glenn, D. B. Bucher, J. Lee, M. D. Lukin, H. Park and R. L. Walsworth, Nature **555**, 351 (2018).
[17] Y. Wu, F. Jelezko, M. B. Plenio, and T. Weil, Angew. Chem. Int. Ed. **55**, 6586 (2016).
[18] A. Bermudez, F. Jelezko, M. B. Plenio and A. Retzker. Phys. Rev. Lett. **107**, 150503 (2011).
[19] J.-M. Cai, B. Naydenov, R. Pfeiffer, L. McGuinness, K. D. Jahnke, F. Jelezko, M. B. Plenio, an A. Retzker, New J. Phys. **14**, 113023 (2012).
[20] M. Hirose, C. D. Aiello, and P. Cappellaro. Phys. Rev. A **86**, 062320 (2012).
[21] J. M. Cai, F. Jelezko, M. B. Plenio and A. Retzker. New J. Phys. **15**, 013020 (2013).
[22] A. A. Maudsley, J. Magn. Reson. **69**, 488 (1986).
[23] G. Uhrig, New J. Phys. **10**, 083024 (2008).
[24] S. Pasini, T. Fischer, P. Karbach, and G. S. Uhrig, Phys. Rev. A **77**, 032315 (2008).
[25] S. Pasini and G. S. Uhrig, J. Phys. A: Math. Theor. **41**, 312005 (2008).
[26] A. M. Souza, G. A. Alvarez, and D. Suter, Phys. Rev. Lett. **106**, 240501 (2011).
[27] Z.-Y. Wang and R.-B. Liu, Phys. Rev. A **83**, 022306 (2011).
[28] A. M. Souza, G. A. Álvarez, and D. Suter, Phil.Trans. R. Soc. A **370**, 4748 (2012).
[29] Z.-Y. Wang, J. F. Haase, J. Casanova, and M. B. Plenio, Phys. Rev. B **93**, 174104 (2016).
[30] J. E. Lang, J. Casanova, Z.-Y. Wang, M. B. Plenio, and T. S. Monteiro, Phys. Rev. Applied **7**, 054009 (2017).
[31] J. F. Haase, Z.-Y. Wang, J. Casanova, and M. B. Plenio, Phys. Rev. Lett. **121**, 050402 (2018).
[32] C. A. Ryan, J. S. Hodges, and D. G. Cory, Phys. Rev. Lett. **105**, 200402 (2010).
[33] B. Naydenov, F. Dolde, L. T. Hall, C. Shin, H. Fedder, L. C. L. Hollenberg, F. Jelezko, J. Wrachtrup, Phys. Rev. B **83**, 081201(R) (2011).
[34] L. M. Pham, N. Bar-Gill, C. Belthangady, D. Le Sage, P. Cappellaro, M. D. Lukin, A. Yacoby, R. L. Walsworth. Phys. Rev. B **86**, 045214 (2012).
[35] L.P. McGuinness, Y. Yan, A. Stacey, D.A. Simpson, L.T. Hall, D. Maclaurin, S. Prawer, P. Mulvaney, J. Wrachtrup, F. Caruso, R.E. Scholten, and L.C.L. Hollenberg, Nature Nanotech. **6**, 358 (2011).
[36] Q.-Y. Cao, Z.-J. Shu, P.-C. Yang, M. Yu, M.-S. Gong, J.-Y. He, R.-F. Hu, A. Retzker, M. B. Plenio, C. Müller, N. Tomek, B. Naydenov, L. P. McGuinness, F. Jelezko, and J.-M. Cai, arXiv:1710.10744.
[37] M. H. Levitt, *Spin dynamics: Basics of nuclear magnetic resonance*, (Wiley, 2008).
[38] M. V. Gurudev Dutt, L. Childress, L. Jiang, E. Togan, J. Maze, F. Jelezko, A. S. Zibrov, P. R. Hemmer, and M. D. Lukin, Science **316**, 1312 (2007).
[39] P. Neumann, J. Beck, M. Steiner, F. Rempp, H. Fedder, P. R. Hemmer, J. Wrachtrup, and F. Jelezko, Science **329**, 542 (2010).
[40] L. Robledo, L. Childress, H. Bernien, B. Hensen, P. F. A. Alkemade, and R. Hanson, Nature **477**, 574 (2011).
[41] T. van der Sar, Z. H. Wang, M. S. Blok, H. Bernien, T. H. Taminiau, D. M. Toyli, D. A. Lidar, D. D. Awschalom, R. Hanson, and V. V. Dobrovitski, Nature **484**, 82 (2012).
[42] G.-Q. Liu, H. C. Po, J. Du, R.-B. Liu, and X.-Y. Pan, Nat. Commun. **4**, 2254 (2013).
[43] S. Kolkowitz, Q. P. Unterreithmeier, S. D. Bennett, and M. D. Lukin, Phys. Rev. Lett. **109**, 137601 (2012).
[44] T. H. Taminiau, J. J. T. Wagenaar, T. van der Sar, F. Jelezko, V. V. Dobrovitski, and R. Hanson, Phys. Rev. Lett. **109**, 137602 (2012).
[45] N. Zhao, J. Honert, B. Schmid, M. Klas, J. Isoya, M. Markham, D. Twitchen, F. Jelezko, R.-B. Liu, H. Fedder, and J. Wrachtrup, Nat. Nanotechnol. **7**, 657 (2012).
[46] B. Hensen, H. Bernien, A. E. Dréau, A. Reiserer, N. Kalb, M. S. Blok, J. Ruitenberg, R. F. L. Vermeulen, R. N. Schouten, C. Abellán, W. Amaya, V. Pruneri, M. W. Mitchell, M. Markham, D. J. Twitchen, D. Elkouss, S. Wehner, T. H. Taminiau, and R. Hanson, Nature **526**, 682 (2015).
[47] I. Lovchinsky, A. O. Sushkov, E. Urbach, N. P. de Leon, S. Choi, K. De Greve, R. Evans, R. Gertner, E. Bersin, C. Müller, L. McGuinness, F. Jelezko, R. L. Walsworth, H. Park, M. D.

Lukin, Science **351**, 836 (2016).
[48] M. H. Abobeih, J. Cramer, M. A. Bakker, N. Kalb, M. Markham, D. J. Twitchen, and T. H. Taminiau, E-Print arXiv:1801.01196.
[49] S. Hartmann and E. Hahn, Phys. Rev. **128**, 2042 (1962).
[50] J. Casanova, Z.-Y. Wang, I. Schwartz, and M. B. Plenio, Phys. Rev. Applied **10**, 044072 (2018).
[51] J. R. Maze, J. M. Taylor, and M. D. Lukin, Phys. Rev. B **78**, 094303 (2008).
[52] See Supplemental Material for further details.
[53] A. Laraoui and C. A. Meriles, Phys. Rev. B **84**, 161403(R) (2011).
[54] B. Naydenov, private communication.
[55] L. Childress, M. V. Gurudev Dutt1, J. M. Taylor A. S. Zibrov, F. Jelezko, J. Wrachtrup, P. R. Hemmer, and M. D. Lukin, Science **314**, 281 (2006).
[56] G. E. Uhlenbeck, and L. Ornstein Phys. Rev. **36**, 36823 (1930).
[57] I. Cohen, N. Aharon, and A. Retzker, Fortschr. Phys. **65**, 1600071 (2017)